Applied Energy 343 (2023) 121208

Contents lists available at ScienceDirect

Applied Energy

journal homepage: www.elsevier.com/locate/apenergy

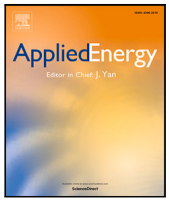

Collective behavior of boreholes and its optimization to maximize BTES performance

Ece Ekmekci [a], Z. Fatih Ozturk [a], Altug Sisman [b,*]

[a] Istanbul Technical University Energy Institute, 34469, Maslak, Istanbul, Turkey
[b] Uppsala University, Department of Physics and Astronomy, Materials Theory Division, Regementsvägen 1, SE-752 37 Uppsala, Sweden

ARTICLE INFO

Keywords:
Borehole thermal energy storage
Ground source heat pumps
Thermal storage efficiency
Configurational effects

ABSTRACT

Borehole layout strongly affects the behavior of borehole heat exchangers (BHEs) and changes the performance of a borehole thermal energy storage (BTES). This study investigates the existence and importance of the optimum collective behavior of BHEs to maximize the performance of BTES. Charge benefit ratio, storage efficiency and configurational benefit factor are proposed as performance indicators for better and finer performance evaluations of BTES systems. A small-scale BTES consisting of ten boreholes arranged on a concentric double-ring layout is considered as an application. Performance variations with the inner and the outer radii of the borehole field are analyzed for the first five years of operation. The temperature fields of different configurations show the transition from collective to individual behavior of boreholes, which leads to an optimal radial configuration maximizing the performance indicators. It is seen that the indicators strongly depend on both inner and outer radii and they reach their maximums for the same distinct radial configuration. The optimum arrangement can almost double the thermal performance indicators. It is thus of great importance to optimize collective behavior to maximize the usage of stored thermal energy. The results are qualitatively general and represent the common behavioral patterns of BTES systems.

1. Introduction

Globally, the residential sector is the third largest energy consumer after the industry and transportation [1] and more than 30% percent of the residential consumption is used for space heating [2]. In addition to such intense thermal energy consumption, the residential sector also contributes to global warming with a substantial amount of greenhouse gas emissions. Therefore, the selection of energy efficient technologies for heating and, if possible, applying renewable energy technologies into the buildings can reduce energy consumption [3] and the environmental impact [4,5]. The energy demand of buildings can be generally grouped as space heating/cooling, domestic hot water and electricity consumption. However, it is obvious that the energy demand of the buildings is also directly dependent on the climatic conditions, thermal properties of the building materials, user behaviors and the energy consumption of electrical devices [6]. Therefore, the modeling of this demand is quite complex due to the changes of these variables for each case and the most importantly changes in user behaviors in time. In the literature, there are engineering, statistical, neural network, machine learning and grey model studies to predict the energy consumption of the buildings [7,8]. These studies not only help to understand the energy performance of buildings but also contribute to efforts for reducing the economic and social impacts of climate change.

The thermal energy demand of buildings mainly arises from domestic hot water and space heating/cooling consumption. This demand can easily be reduced by coupling renewable energy applications to the thermal energy systems and using energy efficient technologies and suitable thermal energy storage systems to store summer heat for winter use. This type of storage system is referred to as long-term thermal energy storage or seasonal thermal energy storage (STES) systems. STES systems use different storage technologies such as sensible, latent and thermochemical heat and each one represents different economic and technical performances [9–12]. One of the most used STES system is the Borehole Thermal Energy Storage (BTES) system which store the thermal energy under the ground using sensible heat storage technologies [13,14]. This technology is generally used by connecting solar thermal panels to the ground source heat exchanger because solar energy is both abundant and available almost in all regions. If the BTES is charged by solar energy, this type of system is called solar-assisted BTES [15]. Furthermore, waste heat from the space cooling in summer seasons or industrial facilities can also be used for charging BTES [16]. Because both solar thermal panels and borehole heat exchangers (BHEs)

* Corresponding author.
E-mail address: altug.sisman@physics.uu.se (A. Sisman).

https://doi.org/10.1016/j.apenergy.2023.121208
Received 13 October 2022; Received in revised form 28 March 2023; Accepted 24 April 2023
Available online 4 May 2023

are modular, BTES are easily applied for both residential and large scale industrial applications [17,18]. Additionally, in this technology, BHEs are also coupled with the heat pump on any scale to improve the temperature difference between underground and the working fluid inside the pump. Finally, all energy storage technologies, both long-term and short-term, create a phase shift between energy demand and consumption. This phase shift is very valuable both for the efficient use of infrastructure by shifting peak hours to off-peak hours and for reducing the energy costs of the end-user.

One of the most important steps in designing the best BTES is the correct determination of the thermophysical properties of the ground for calculating the heat transfer rate between the ground and heat exchangers. The most used method in determining the thermophysical properties of the ground is the thermal response test (TRT) [19–21]. In this method, usually the average thermal properties of the ground are obtained for a homogenized ground by using the differences between the inlet and outlet fluid temperatures of the ground heat exchanger and the mass flow rate. On the other hand, underground is an in-homogeneous structure with mostly layered formations, clearly, the thermophysical properties of each layer may differ significantly from each other. Therefore, in order to get more detailed information about the thermophysical properties of the ground at different depths, the distributed thermal response test method is developed with the help of optical fiber thermometers [22,23]. Because the homogeneous model simply treats all layers as a single layer with averaged properties, there may be considerable differences in modeling and computation time between the homogeneous and the layered models. Even the shallow vertical heat exchangers may pass through different layers under the ground, there are many studies evaluating the performance of heat exchangers in layered structures [24–26]. However, when the thermal performances of BHEs are computed using the thermo-statistical properties of the underground layers, the differences between the performance predictions of the BHEs based on homogeneous and layered models are less than 3% since the interlayer heat transfer is negligible for almost all cases [27] and such small differences make the homogenized model easily applicable and usually favorable. Furthermore, Lou et al. [28] examined performance of the BHE for five layers ground using homogeneous and non-homogeneous approach and found almost the similar thermal outputs. The Optimal BHE configuration for a BTES application can completely be different than that of a conventional BHE field without thermal energy storage, because, the thermal shortcuts reduce the performance of conventional BHEs [29] while the collective behavior can even improve the performance of a system with BTES.

BTES performance can be optimized by taking many different parameters into account, such as design, material and operating parameters. BTES systems having different design characteristics, climatic conditions and heat sources, are actively used all over the world [30]. By considering the combinations of the various numbers of BHEs having different depths, spacing, inlet and outlet temperatures as well as underground properties, Welsch et al. [31] investigated the performance of 250 different medium deep BTES configurations in which BHEs are placed on a concentric circular layout with a constant spacing for each different depths of BHEs and they showed that there is an optimum BHE spacing for each case. Lundh and Dalenback [32] studied well-known BTES project of 100 BHEs for 50 residential unit in Sweden and decided that it was appropriate to place the BHEs with 3 meters spacing in a quadratic cross section. Woloszyn [33] investigated the global sensitivity of BHEs arrangement to maximize the system performance by changing the lateral distances and the inclination angle of BHEs, and the maximum efficiency has been reached for the lateral distances in the range of 1.5–3 m with the inclination angle of 0°. Different from the ground source heat pump applications, in BTES systems, a thermal insulation layer is usually applied near the ground surface to prevent heat leakage into the atmosphere. Also, waterproof materials are generally chosen for the insulation layer to avoid surface water penetration causing both evaporative and convective energy losses from the BTES region. This practically stops the heat exchange from the top of the BTES application field. Thus, the stored heat is prevented from leaving the storage area to improve the system's performance [34]. Furthermore, in the case of ground source heat pump applications, Bidarmaghz et al. [35] studied the effects of changes in air temperature on their performance and showed that even for 50 m deep BHEs, the atmospheric effects reduce the performance only about 6%. Ma et al. [36] experimentally investigated laboratory scale storage system by changing soil properties, flow rates and temperature of working fluid and intensity of radiation, and found that the soil water saturation degree increases the energy storage per unit length of borehole and the saturated soil shows more uniform temperature profiles.

In this study, a small-scale BTES for 5–20 houses is considered since it is one of the most common application scales. Due to the small number of BHE, a circular geometry is chosen for the layout of BHEs to minimize the outer surface-to-volume ratio of BTES field and keep the heat leakages from the field at the lowest. When the application scale becomes much larger, naturally, the shape of the layout geometry of BHE becomes practically unimportant as the surface-to-volume ratio already becomes too small. Therefore, for large-scale applications consisting of a few hundred to thousands BHE, rectangular or hexagonal layout geometries are also quite reasonable options. For the small-scale applications studied here, a BTES consisting of ten BHEs (1 + 3 + 6) arranged on a concentric double-ring geometry is considered. BHE depth is chosen as 50 m and it can be chosen deeper depending on the total heat demand, i.e. the number and the size of the houses connected to this system. On the other hand, the results are practically not affected by the depth of BHEs since the dominant heat transfer direction is the radial one. The number of BHE on the outer ring is chosen as the double of the ones on the inner ring to absorb most of the heat leaked away from the encircled region. Installation of unnecessarily many BHEs on the outer ring not only increases the BTES cost but also even might increase the heat leakages because of the increased heat diffusion toward the outside of the outer ring. Therefore, 1 + 3 + 6 BHE combination is chosen as a small-scale BTES and the various inner and outer radii combinations are studied to uncover the existence and the importance of the optimal collective BHE behavior maximizing the thermal performance of BTES. The sensitivity of BTES performance to the optimal configuration is also shown. The optimal collective behavior determining the best layout configuration is naturally expected also for other layout geometries and large-scale applications. In this context, qualitative results are general and represent the common behavioral patterns of BTES systems.

Welsch et al. comprehensively analyzed the effects of various parameters on the performance of a BTES, while the performance changes due to different combinations of inner and outer radius for a constant number of BHEs remained untouched. Different from the study by Welsch et al. [31], here we investigate how thermal performance and the collective behavior of a small-scale BTES field change with the sizes of circular layout when the number of BHEs and all other parameters remain constant. The charge and discharge durations of BTES are determined by considering the local climate condition. The average underground thermophysical properties are used for the calculation of heat transfer rates since the difference between the predictions of layered and homogenized models is negligible as mentioned before.

Furthermore, in the literature, the thermal recovery factor is commonly used as a measure of energy storage efficiency. It is defined as the ratio of the extracted energy to the stored (charged) one. On the other hand, since the temperature of circulating fluid in a heat pump connected BHE is usually able to go below the undisturbed ground temperature, the extracted energy is generally a combination of both charged and the already available thermal energy in the ground. Thus, it is always possible to extract thermal energy from the ground even if it is not charged before. Because of that, the recovery factor does not reflect the true performance of energy storage and recovery processes. The less the charge the higher the recovery factor and in the case

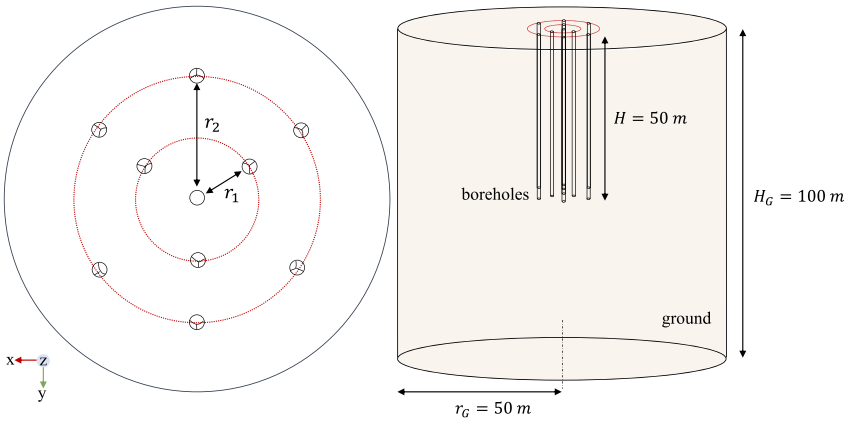

Fig. 1. The layout of borehole heat exchangers: the top view is on the left and the perspective view is on the right.

of zero charge, the recovery factor even goes to infinity and causes misconception and confusion. Therefore, although the recovery factor in the literature is a helpful quantity it does not represent the true storage efficiency. To determine how much percentage of the charged energy is truly recovered from the ground, it is important to know how much energy could be discharged (extracted) from BTES if the system had not been charged. In this study, also an alternative storage efficiency expression based on the storage energy usage is proposed for a better representation of the storage performance of a BTES. Charge benefit ratio and configurational benefit factor are also proposed for better and finer performance evaluations of BTES. The variations of these performance indicators with the radial sizes of circular arrangement are analyzed to find the optimum configuration to maximize BTES performance.

The main job of the study is to optimize the collective behavior of BHEs and hence the borehole density distribution (arrangement) to maximize the proposed performance parameters. However, because the optimum distribution depends on many parameters such as ground properties, charge–discharge periods, number of boreholes, etc., a computational simulation is the best way to prevent a possible inaccurate design and arrangement of BHEs. When we consider today's computer performances, the computer simulations based on numerical methods, like FEM, are quite reasonable for BTES analyses under BHEs mutual thermal interactions. There are some semi-analytical methods to determine the mutual interactions of BHEs, like the cross g-functions [37]. On the other hand, they also need the numerical calculations of too many integrals when the number of BHEs becomes higher and hence results in also some calculation loads. Independent of which method is used, the results are the same since the solution necessarily be unique. Here, the numerical simulations based on FEM in the Comsol environment are preferred.

2. Model

2.1. Model description

A small-scale BTES field consisting of ten BHEs, each 50 m depth, is considered. One of the BHEs is positioned in the center of a concentric double-ring configuration, while three and six BHEs are located on the inner ring of radius r_1, and the outer ring of radius r_2 respectively as seen in Fig. 1. Variations of thermal performance indicators with radial sizes of the BHEs layout are numerically investigated for the first five years of operation. During the examinations, the radius ratio is first kept constant as, $r_2/r_1 = 2$ while the radius of the inner ring is changed in between 1–12 m. Later, the ratio is changed in the range of 1.33 to 5 while $r_1 = 3$ m.

In the numerical model, the depth and diameter of the ground environment are chosen so large that the boundaries do not affect the simulation results in both radial and vertical directions. Due to the thermal insulation layer application near the ground surface in BTES fields, the isolation boundary condition is applied to the top surface of the storage system. The city of Erzurum/Turkey is chosen as an application field for BTES and the undisturbed ground temperature T_∞ is approximated by the mean annual air temperature of the city as 5.7 °C. This is the value used as the initial condition at the beginning of the numerical calculations. This common approach [38] is also confirmed for another city in Turkey by measuring T_∞ at different depths in the heat pump field laboratory of the Energy Institute of Istanbul Technical University, and it is observed that the relative error of the approach is approximately 4% [39]. The BTES is operated in both charge and discharge modes. There are also standby modes in between charge and discharge processes.

The main motivation of the study is to show the existence of optimal collective behavior to maximize the thermal performance parameters of BTES. The real data-based scenario can be applied to the model to see the results for a specific year. On the other hand, the results become case-dependent since the atmospheric data is different for each year. To consider the worst-case scenario, we choose the lowest practical temperature for the borehole surfaces during the discharge period and the daily average charge temperature for the summer period. A constant boundary surface temperature condition is used if the seasonally averaged BHE surface temperature can be estimated. The average BHE temperature is determined not only by the seasonal amounts of heat demand and heat supply, which depend on air temperature and solar radiation data respectively, but also by the number of BHEs and their depths as well as the number of houses and installed thermal power of solar collectors. Therefore, it is possible to adjust the control and design parameters of the problem to use specific values for constant boundary temperatures. The constant temperature boundary condition considerably decreases the computing time for optimization scenarios. In our case, the numerical calculations become two times faster in comparison with the case of variable boundary conditions based on hourly atmospheric data. The small difference between inlet and outlet fluid temperatures makes the constant temperature boundary condition for borehole surfaces technically applicable for axial direction as well. Note that this temperature difference can also be adjusted by changing the flow rate.

In the charge mode, hot water from a thermal mixing and accumulation tank, charged by a solar thermal system, is pumped directly to the BHEs at 40 °C while the heat pump is off. In this way, heat energy is transferred to the ground from the borehole surfaces kept at 40 °C. In the discharge mode, the heat pump is operated and thermal energy including some part of the stored one is pumped from the ground to the heated space. As a worst case scenario, the temperature difference between the undisturbed ground and the borehole surface is chosen as 15 °C, therefore, the borehole surface temperature is kept constant at

Table 1
Design and operational parameters of BTES and thermal properties of the ground.

Number of boreholes N (1 + 3 + 6),	10
Depth of boreholes, H	50 m
Radius of boreholes, r_B	0.1 m
Ground depth in the model, H_G	100 m
Ground radius, r_G	50 m
Undisturbed ground temperature, T_∞	5.7 °C
Borehole surface temperature in discharge mode, T_B^{DC}	−9.3 °C
Borehole surface temperature in charge mode, T_B^C	40 °C
Ground thermal conductivity, k	2.14 W m/K
Ground density, ρ	2500 kg/m^3
Ground specific heat capacity, c_p	858 J/kg K
Ground thermal diffusivity, α	9.98 × 10^{-7} m^2/s
Charging duration	3 months
Discharging duration	8 months
Standby duration after discharge and charge modes	15 days

−9.3 °C during the discharge mode. All the system parameters including the thermophysical properties of the ground, lengths and radius of the boreholes, design temperatures, charge and discharge durations are given in Table 1. Due to the climatic conditions of the city, the discharge duration is much longer than the charge duration.

Furthermore, in large-scale BTES systems, inner boreholes can be used for charging and outer boreholes for discharging. However, in small-scale systems consisting of a small number of BHEs, it is not economically feasible to add some extra boreholes used only for the discharge process, when we consider the drilling costs and practically cost-free solar energy for the charging process. Therefore, all BHEs in this study are used both in charge and discharge periods.

Thermophysical properties of the ground are assumed to be homogeneous and isotropic. Because the dependency of thermophysical properties on temperature is smooth and the variations of ground temperature during the charge and discharge processes remain in a limited range, there is no noticeable change in these quantities for the studied temperature range. Therefore, the thermophysical properties are considered as constant quantities.

3D finite element method is implemented to solve the transient heat diffusion equation for BTES field to determine the temperature profiles around BHEs and heat transfers. A commercial software environment, COMSOL, is used and approximately 175 k – 240 k tetrahedral meshes are generated depending on the outer radius of BHE field. The following transient heat diffusion equation is considered for BHEs to calculate the thermal energy transfers during each process,

$$\frac{1}{\alpha}\frac{\partial T}{\partial t} = \frac{\partial^2 T}{\partial r^2} + \frac{1}{r}\frac{\partial T}{\partial r} + \frac{\partial^2 T}{\partial z^2}, \tag{1}$$

where; α is thermal diffusivity, T is temperature, t is time, r is the radial distance from the center of a borehole and z is the depth from the ground surface. The thermal diffusivity coefficient is determined as $\alpha = k/\rho c_p$, where, ρ is the density, c_p is the specific heat capacity and k is the thermal conductivity coefficient of the ground. The undisturbed ground temperature increases with depth in general and this becomes important for deep BHE applications. On the other hand, the considered BHEs have only 50 m depth, and therefore, the depth-dependency of initial ground temperature is negligible. However, the finite depth of BHEs causes edge effects which locally destroy the symmetry of the problem and needs 3D treatment. The 3D domain is discretized using the integrated mesh generator of COMSOL software and the meshes are refined in the vicinity of all BHE surfaces until the numerical results exhibit a mesh-independent temperature profile. In between the discharge (DC) and charge (C) periods, there are standby (SB) periods as well. Annual cycles are in the order of DC–SB–C–SB. Durations of DC, SB and C periods are determined by considering the monthly averaged temperatures of the city. Eq. (1) is numerically solved for the considered BHE field under the initial and boundary conditions given as follows for DC, SB and C periods respectively expressed by Eqs. (2a)–(2c):

$$\begin{aligned}&\text{Discharge mode}: 0 \le t \le t_{DC}, \quad T_{DC}(r,z,0) = T_\infty \\ &T_{DC}(r_B, z \le z_B, t) = T_{DC}(r \le r_B, z_B, t) = T_B^{DC}, \quad T_{DC}(r_G, z, t) = T_\infty \\ &\left(\frac{\partial T_{DC}(r,z,t)}{\partial z}\right)_{z=0} = 0, \quad T_{DC}(r, H_G, t) = T_\infty\end{aligned} \tag{2a}$$

$$\begin{aligned}&\text{Standby mode}: t_{DC} \le t \le t_{SB}, \quad T_{SB}(r,z,t_{DC}) = T_{DC}(r,z,t_{DC}) \\ &\left(\frac{\partial T_{SB}(r,z,t)}{\partial r}\right)_{\substack{r=r_B \\ z\le z_B}} = \left(\frac{\partial T_{SB}(r,z,t)}{\partial r}\right)_{\substack{r\le r_B \\ z=z_B}} = 0, \quad T_{SB}(r_G,z,t) = T_\infty \\ &\left(\frac{\partial T_{SB}(r,z,t)}{\partial z}\right)_{z=0} = 0, \quad T_{SB}(r, H_G, t) = T_\infty\end{aligned} \tag{2b}$$

$$\begin{aligned}&\text{Charge Mode}: t_{SB} \le t \le t_C, \quad T_C(r,z,t_C) = T_{SB}(r,z,t_{SB}) \\ &T_C(r_B, z \le z_B, t) = T_C(r \le r_B, z_B, t) = T_B^C, \quad T_C(r_G, z, t) = T_\infty \\ &\left(\frac{\partial T_C(r,z,t)}{\partial z}\right)_{z=0} = 0, \quad T_C(r, H_G, t) = T_\infty\end{aligned} \tag{2c}$$

The difference between the surface temperature of BHEs and the mean fluid temperature in U-tubes is in the order of a few degrees. The transient temperature process inside the BHE radius is completed within hours (12–48 h) depending on the structure of BHE while the operation periods are in months for C and DC modes and in weeks for SB. Therefore, BHEs are considered as hollow cylinders with a constant surface temperature. The heat transfer rate on the surface of each borehole is calculated from the temperature field by

$$\dot{Q} = -k \int_0^H 2\pi r_B \left(\frac{\partial T}{\partial r}\right)_{r=r_B} dz \tag{3}$$

where H is the depth of the BHE and the total heat energy transfer of a single borehole is obtained by

$$Q = \int_0^t \dot{Q}(t')\, dt' \tag{4}$$

The total heat rate, $\sum_{i=1}^N \dot{Q}_i(t)$, and the total heat energy transfer, $\sum_{i=1}^N Q_i(t)$, are simply obtained by summing over the each BHE values where N is the borehole number in BTES. Using Eqs. (3)–(4) the charged, Q_C, and discharged, Q_{DC}, amounts of heat energy are numerically calculated for the first five years of BTES operations. The amount of heat energy that can be absorbed from the ground during the discharge process without any prior charging process, Q_{DC}^{WC}, is also determined.

2.2. Model validation

In order to validate the numerical models, problems are usually solved by more than one numerical method or the results are directly compared with the analytical solutions [40]. When all the BHEs of BTES in this study are far enough from each other, the total amount of extracted energy from the ground simply converges to the one for a single BHE multiplied by the total number of BHEs. Therefore, such a case allows us to verify the numerical model because there is already an analytical solution in literature for the radial heat flux of a single BHE considered as a hollow cylinder with constant temperature boundary condition, [41]. On the other hand, other analytical models such as finite-length linear heat-source [42] or finite cylinder-source [43] models may also be used for the model validation.

Therefore, the results of the numerical model are compared with the analytical ones for the period of 5760 h during the discharge process of the first year when $r_1 = 12$ m and $r_2 = 24$ m, which makes the interactions between BHEs negligible. The mean absolute percentage errors (MAPE) for the heat rate and the heat energy transfer are calculated as %3.0 and % 3.2, respectively for the used mesh

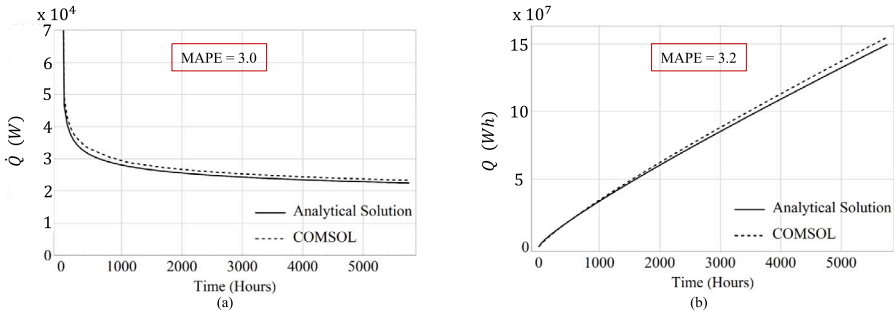

Fig. 2. Comparison of the analytical and numerical results for (a) heat rate and (b) heat energy transfer.

structure in this study. MAPE values can even be further reduced simply by increasing the mesh number if the computation time is not an issue. The heat rate and heat energy transfer for each BHE are analytically given as [27,44],

$$\dot{Q}(t) = 2\pi(T_B^{DC} - T_\infty)Hk\frac{4}{\pi^2}\int_{\beta=0}^{\infty}\frac{\exp\frac{-\beta^2\alpha t}{r_B^2}}{\beta[J_0^2(\beta)+Y_0^2(\beta)]}\,d\beta \tag{5}$$

$$Q(t) = 2\pi r_B^2 H(T_B^{DC} - T_\infty)\rho c_p\frac{4}{\pi^2}\int_{\beta=0}^{\infty}\frac{1-\exp\frac{-\beta^2\alpha t}{r_B^2}}{\beta^3[J_0^2(\beta)+Y_0^2(\beta)]}\,d\beta \tag{6}$$

where; J_0 and Y_0 are the first and the second kind of zeroth order of Bessel functions respectively, t is the time in discharge mode. The analytical and numerical results, including MAPE values, are compared in Fig. 2.

3. Results

Due to the unavoidable heat leakage to the regions away from BTES field, the stored thermal energy cannot fully be recovered from the ground. Therefore, in order to determine the net benefit of a BTES and its limits, first the total amount of discharged energy from the BHE field is calculated without any prior charging (WC) process as a reference quantity. For this case (WC), charging period is added to the stand-by period since there is no charging process. Consequently, in this reference case, heat energy is discharged from the ground for eight months and then the heat exchange process is paused for four months in standby mode. This cycle continues for five successive years of operation and the discharged energy without any charging process is represented by Q_{DC}^{WC}. Five-years operations start with discharge mode. For this reference case, the extracted energy from BHEs decreases during the years since there is not enough time to recover the undisturbed ground temperature in the vicinity of BHEs. Therefore, the mean surface temperature of BHEs just before the discharge process, $\overline{T}_B^{bDC}$, decreases over time and goes below the undisturbed ground temperature, $T_\infty = 5.7$ °C, as seen in Fig. 3-a. But this decrement slows down by years because the decreasing $\overline{T}_B^{bDC}$ increases the temperature differences between BHE surface and the undisturbed ground temperature and it improves the heat transfer rate as well as the recovery time of the temperature profile. The worse case is achieved for $r_1 = 3$ m, which maximizes the discharged energy. If the BTES is charged, however, $\overline{T}_B^{bDC}$ considerably increases and becomes even time-independent and also takes the values much higher than T_∞ for all values of r_1. The mean surface temperature of BHEs just before charging, $\overline{T}_B^{bC}$, also becomes time-independent and increases for higher values of r_1 as seen in Fig. 3-b.

The temperature fields of the ground around a single borehole and multi-borehole BTES are given in Fig. 4. These temperature distributions provide important information about the transition from collective to individual behavior of BTES field with increasing distances between BHEs. Fig. 4-a shows the temperature distribution around a single borehole BTES at the end of the first five years of operation. The thermophysical properties of the ground are homogeneous and the heat diffusion is isotropic in the domain, therefore, the isotherms normally show circular characteristics. However, for multi-BTES, interactions cause collective behavior and isotherms cover the larger areas with higher temperatures when BHEs are relatively close to each other, Fig. 4b–d. On the other hand, collective behavior starts to decay and the individual behavior becomes more and more apparent while the distance between BHEs increases, Fig. 4e–f. Eventually, the collective behavior is totally lost and the configurational benefit almost disappears since the interactions become negligible due to over distance between BHEs, Fig. 4 g–i. The performance values of multi-BTES are different from each other for each configurational radius. In this study; the charge benefit ratio, the configurational benefit factor and the storage efficiency definitions are introduced to compare the BTES performances for different values of the radius. The ratio of discharged energy, Q_{DC}, to the one without prior charging, Q_{DC}^{WC}, is described as the charge benefit ratio and written as,

$$\hat{Q}_{CB} = \frac{Q_{DC}}{Q_{DC}^{WC}} \tag{7}$$

The variations of charge benefit ratio with time and configurational radius are given in Fig. 5. Note that both r_1 and r_2 change simultaneously while their ratio remains constant as $r_1/r_2 = 2$. Although the charge benefit ratios are calculated for nine different radii, due to the similar characteristics of the curves, the only ones for three different radii are shown together with that of a single borehole in Fig. 5a. In conventional ground source heat pump applications, if the BHE field is sufficiently large, the BHEs are placed far away from each other to prevent thermal shortcuts between the BHEs and improve thermal performance. In other words, in a conventional BHE field, it is the desired condition that each BHE in the field behaves individually. In the case of BTES, however, the desired condition is different. From both figures in Fig. 5, the most advantageous configuration is achieved when $r_1 = 3$ m. Therefore, the shorter or longer configuration radius clearly decreases the performance of a multi-BTES. Consequently, there is an optimum radius for the concentric circular configuration of multi-BTES. It is also seen from Fig. 5a that variations of charge benefit ratio with both time and configuration radius show asymptotic behaviors. In Fig. 5-b, the charge benefit ratio approach to its single BHE value when r_1 getting larger and larger values which destroy the collective behavior.

Another performance indicator is the configurational benefit factor proposed and defined here as,

$$f_{CB} = \frac{\hat{Q}_{CB}}{\hat{Q}_{CB}^{SB}} \tag{8}$$

where; $\hat{Q}_{CB}^{SB}$ is the charge benefit ratio of BTES with a single BHE. Eq. (8) represents the benefit just because of the collective behavior. Its variations with time and radius are seen in Fig. 6. Almost all the comments made for Fig. 5 are also valid for Fig. 6. In addition, in Figs. 5-b and 6-b, it is seen that the performance values rapidly decrease

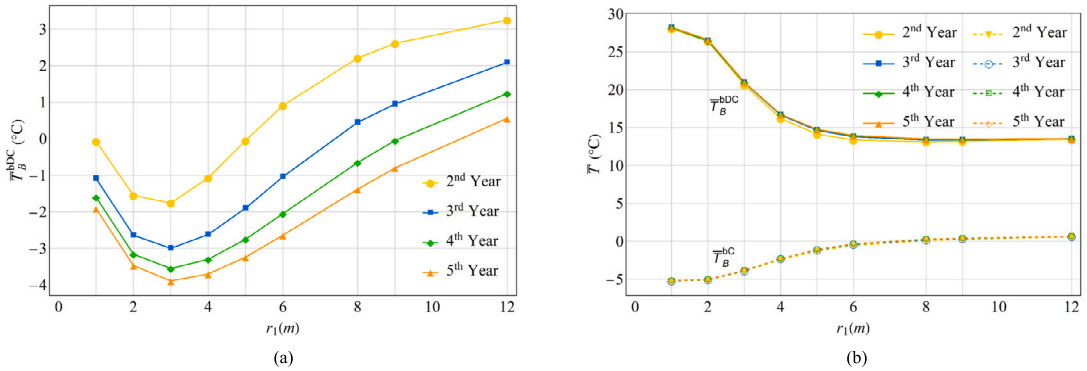

Fig. 3. Variation of the mean surface temperature of BHEs with the inner radius just before the charge and discharge modes (a) without prior charging and (b) with charging. Note that $r_2/r_1 = 2$.

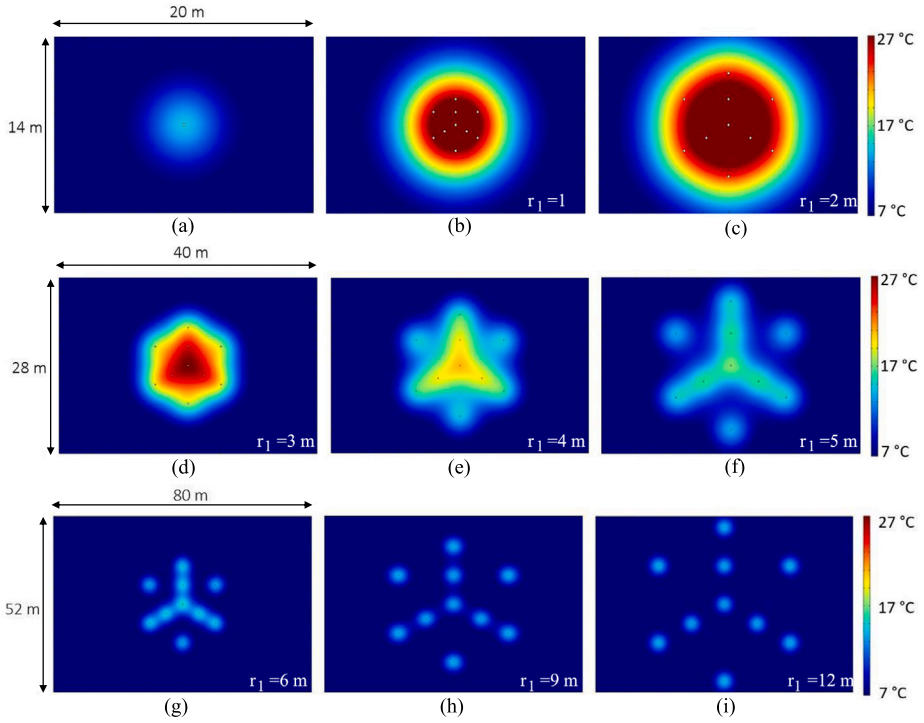

Fig. 4. Temperature distributions at the end of five years of operation for different inner radius of BHEs layout: (a) a single borehole and (b–i) 10-boreholes. Note that $r_2/r_1 = 2$ and $T_\infty = 5.7$ °C.

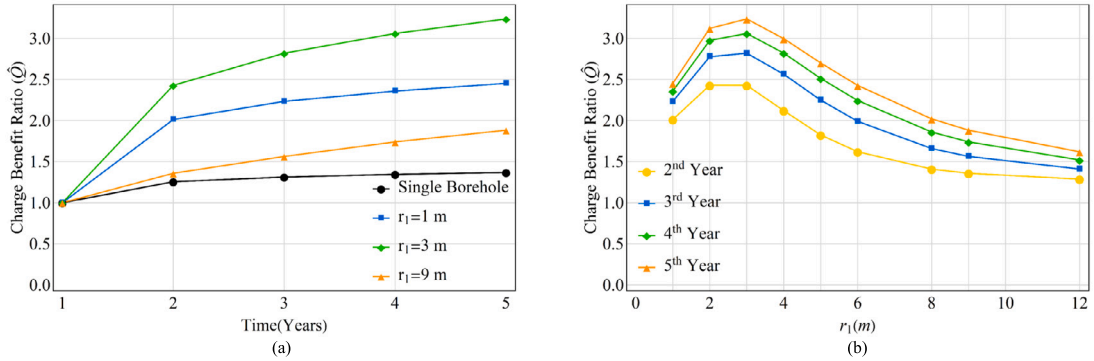

Fig. 5. Variation of charge benefit ratio with (a) operation time and (b) the inner radius. Note that $r_2/r_1 = 2$.

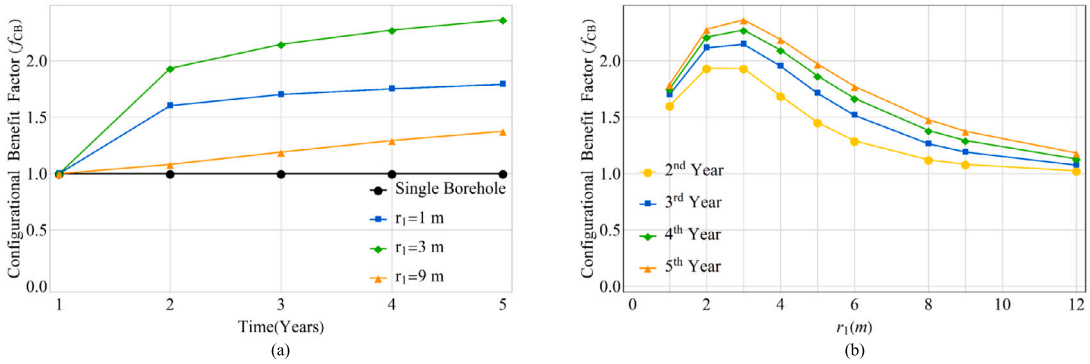

Fig. 6. Variation of configurational benefit factor with (a) operation time and (b) the inner radius. Note that $r_2/r_1 = 2$.

when the distance between the BHEs falls below the optimum radius of 3 m. If the radius is further reduced so that the BHEs form a close bundle, BTES behaves as a large quasi-single BHE with lower configurational benefit factor.

The storage efficiency may be the most informative indicator for thermal energy storage systems. The recovery factor is commonly used as a thermal performance indicator of BTES and is defined as the ratio of extracted energy to charged energy. On the other hand, since the temperature of circulating fluid in a heat pump connected BHE can go below the undisturbed ground temperature, the extracted energy is usually a combination of both charged and the already available thermal energy in the ground. In other words, since there is always usable thermal energy already in the ground even if it is not charged before, the recovery factor does not reflect the true performance of the storage process and the percentage of charged energy usage during a discharge process. In the case of zero charge, the recovery factor even goes to infinity and causes misconception and confusion. To determine the how much stored energy is used, it is important to know how much energy could be discharged from BTES if the system had not been charged. For this purpose, by keeping all the conditions the same, the discharge energy without a prior charge process is also determined. As a result of this information, the storage efficiency of BTES is introduced here as,

$$\eta = \frac{Q_{DC} - Q_{DC}^{WC}}{Q_C} \tag{9}$$

In short, the storage efficiency is defined as the stored energy usage per charged energy where $Q_{DC} - Q_{DC}^{WC}$ is the stored energy usage computed as the difference between the discharged energies with and without prior charging processes. Note that the storage efficiency properly goes to zero in the case of zero charge and serves as a true indicator for storage efficiency of a BTES. The variation of the storage efficiencies with time and various radii are given in Fig. 7. The highest efficiency value is obtained for $r_1 = 3$ m and at the end of the fifth year the efficiency reaches almost 2.5 times higher value than that of a single borehole BTES. The existence of an optimum spacing for thermal performance indicators generally agrees with the results given by Welsch et al. [31].

The variations of three performance indicators with the radius ratio are also examined for a constant inner radius, $r_1 = 3$ m. In Fig. 8, we see that both the charge benefit ratio and the configurational benefit factor have similar characteristics and they reach their maximum values when $r_2/r_1 = 1.67$. This shows that the configuration of $r_1 = 3$ m, $r_2 = 5$ m is the global maximum in (r_1, r_2) plane. The dependency of the storage efficiency on radius ratio in Fig. 9 also confirms the existence of this global maximum. It is seen that the storage efficiency changes smoothly in Fig. 9 in comparison with Fig. 7. This is because all BHEs move away from each other when we increase r_1 while $r_2/r_1 = 2$ in Fig. 7. On the other hand, in Fig. 9, we keep the BHEs on the first ring constant as $r_1 = 3$ m and change only the ones on the second ring. It should be noted that, however, the optimum values of r_1 and r_2 always depend on ground properties, chosen layout geometry (here it is the concentric double-ring), charge/discharge temperatures and the local climate conditions which determine also the charge and discharge periods.

4. Conclusion

Examinations of configurational size effects on proposed performance indicators showed that there is an optimum radial configuration that maximizes the benefits of collective behavior of BHEs in a BTES field. Each performance indicator asymptotically increases throughout the first five years of operation. However, the optimum configuration radius is almost the same for all indicators and it provides the maximum thermal performance for a small-scale concentric double-ring BTES field. The optimum arrangement can almost double the thermal performance indicators as seen from Figs. 5b–7b. The best configuration is $r_1 = 3$ m, $r_2 = 6$ m for thermal and operational conditions considered here. For the radii below and above these optimal values, the collectively behaved field becomes smaller and the performance indicators decrease. This leads to the loss of a considerable amount of stored energy. Therefore, the optimization of the collective behavior of BHEs in a BTES has an essential effect on thermal performance. It becomes even more important for small-scale BTES applications consisting of dozens of BHEs.

The results are qualitatively general and represent the common behavioral patterns of BTES systems, particularly the small-scale ones. Quantitatively, the increment of BHEs on the inner and outer rings does not affect the optimum configuration as long as the distance between BHEs is not practically less than the thermal interaction coefficient. The value of the interaction coefficient is around 3 m for isotropic BHE distribution and the long operation times considered here, [29]. For example, instead of 1 + 3 + 6 BHEs, if 1 + 6 + 12 combination is considered, the optimum radial configuration remains the same as $r_1 = 3$ m and $r_2 = 6$ m. On the other hand, the charge benefit ratio and the configuration benefit factor improve from 3.2 and 2.4 to 4.4 and 3.2 respectively and the storage efficiency rises from 72% to 78%. On the contrary, the depth of BHEs practically neither affects the optimum configuration nor the results since the dominant heat transfer direction is the radial one.

It seems that the thermal interaction coefficient plays an important role to determine the best configuration (arrangement) of BHEs for the optimum collective behavior maximizing the thermal performance of BTES. Instead of double rings, if triple, quadruple or more rings are considered, the possible best configuration becomes $r_1 = 3$ m, $r_2 = 6$ m, $r_3 = 9$ m,... if the thermal interaction coefficient is around 3 m and the distance between BHEs is not smaller than this value. By keeping these conditions, if we increase the number of BHEs on each ring, we increase the performance indicators.

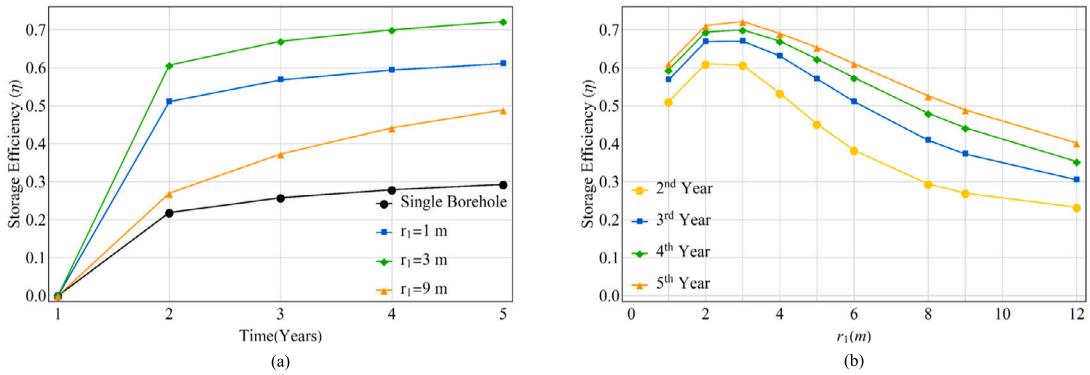

Fig. 7. Variation of the storage efficiency with (a) operation time and (b) the inner radius. Note that $r_2/r_1 = 2$.

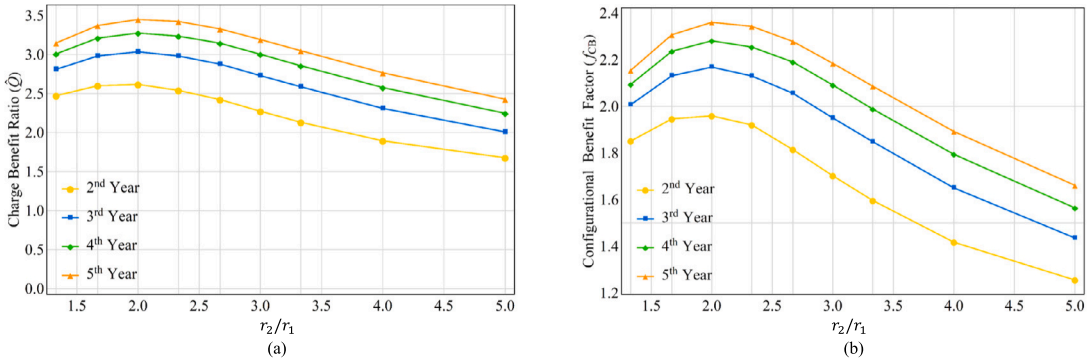

Fig. 8. Variations of (a) charge benefit ratio and (b) and the configurational benefit factor with the radius ratio, r_2/r_1. Note that $r_1 = 3$ m.

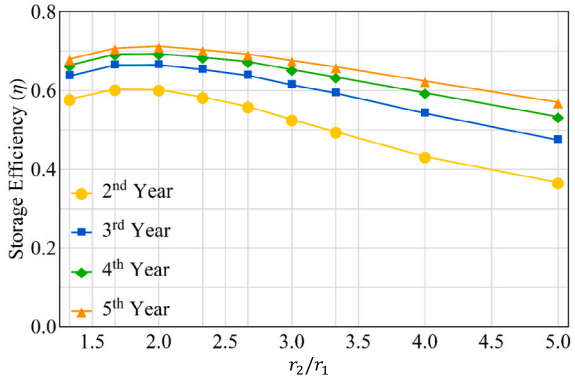

Fig. 9. Variations of the storage efficiency with the radius ratio, r_2/r_1. Note that $r_1 = 3$ m.

On the other hand, the thermal properties of the ground as well as the durations and the temperatures of charge and discharge modes determine the strength of thermal interactions between BHEs. Therefore, the interaction coefficient and hence the optimal configuration and the performance indicators change when these thermal and operational parameters considerably change.

For ground source heat pump applications, the best performance is achieved when the distance between BHEs is much larger than the thermal interaction coefficient. For BTES applications, however, the best performance is obtained when the distance is around the thermal interaction coefficient.

The main goal is to recover as much of the charged energy as possible and increase the thermal performance indicators. Arranging the same number of boreholes at different distances or geometries clearly affects the performance. Optimal BTES configuration is also affected by the thermophysical properties of the ground and the charge/discharge durations of the field. If the ground properties are homogeneous and isotropic, the angular symmetric BHE arrangements generally provide the highest configurational benefit factor for some optimal sizes. But, if there is ground water flow, this flow constitutes a preferential direction for the heat transfer, and under such conditions, the deformed geometries, like ellipse, for BHE layout may provide the highest configurational benefit factor.

The effects of the number density of BHEs in each ring and the ground water flow on the performance indicators are possible extensions of the study. These problems are now under consideration by the same research group.

CRediT authorship contribution statement

Ece Ekmekci: Formal analysis, Validation, Visualization. **Z. Fatih Ozturk:** Conceptualization, Writing – original draft, Investigation. **Altug Sisman:** Conceptualization, Methodology, Supervision, Writing – review & editing.

Declaration of competing interest

The authors declare that they have no known competing financial interests or personal relationships that could have appeared to influence the work reported in this paper.

Data availability

No data was used for the research described in the article.

References

[1] Nejat P, Jomehzadeh F, Taheri MM, Gohari M, Abd. Majid MZ. A global review of energy consumption, CO2 emissions and policy in the residential sector (with an overview of the top ten CO2 emitting countries). Renew Sustain Energy Rev 2015;43:843–62. http://dx.doi.org/10.1016/j.rser.2014.11.066.

[2] Ürge-Vorsatz D, Cabeza LF, Serrano S, Barreneche C, Petrichenko K. Heating and cooling energy trends and drivers in buildings. Renew Sustain Energy Rev 2015;41:85–98. http://dx.doi.org/10.1016/j.rser.2014.08.039.

[3] Song J, Oh S-D, Song SJ. Effect of increased building-integrated renewable energy on building energy portfolio and energy flows in an urban district of Korea. Energy 2019;189:116132. http://dx.doi.org/10.1016/j.energy.2019.116132.

[4] Vares S, Häkkinen T, Ketomäki J, Shemeikka J, Jung N. Impact of renewable energy technologies on the embodied and operational GHG emissions of a nearly zero energy building. J Build Eng 2019;22:439–50. http://dx.doi.org/10.1016/j.jobe.2018.12.017.

[5] Carvalho AD, Mendrinos D, De Almeida AT. Ground source heat pump carbon emissions and primary energy reduction potential for heating in buildings in Europe—results of a case study in Portugal. Renew Sustain Energy Rev 2015;45:755–68. http://dx.doi.org/10.1016/j.rser.2015.02.034.

[6] Vivian J, Chiodarelli U, Emmi G, Zarrella A. A sensitivity analysis on the heating and cooling energy flexibility of residential buildings. Sustainable Cities Soc 2020;52:101815. http://dx.doi.org/10.1016/j.scs.2019.101815.

[7] xiang Zhao H, Magoulès F. A review on the prediction of building energy consumption. Renew Sustain Energy Rev 2012;16(6):3586–92. http://dx.doi.org/10.1016/j.rser.2012.02.049.

[8] Amasyali K, El-Gohary NM. A review of data-driven building energy consumption prediction studies. Renew Sustain Energy Rev 2018;81:1192–205. http://dx.doi.org/10.1016/j.rser.2017.04.095.

[9] Yang T, Liu W, Kramer GJ, Sun Q. Seasonal thermal energy storage: A techno-economic literature review. Renew Sustain Energy Rev 2021;139:110732. http://dx.doi.org/10.1016/j.rser.2021.110732.

[10] Xu J, Wang R, Li Y. A review of available technologies for seasonal thermal energy storage. Sol Energy 2014;103:610–38. http://dx.doi.org/10.1016/j.solener.2013.06.006.

[11] Pavlov GK, Olesen BW. Thermal energy storage—A review of concepts and systems for heating and cooling applications in buildings: Part 1—Seasonal storage in the ground. HVAC R Res 2012;18(3):515–38. http://dx.doi.org/10.1080/10789669.2012.667039.

[12] Hesaraki A, Holmberg S, Haghighat F. Seasonal thermal energy storage with heat pumps and low temperatures in building projects—A comparative review. Renew Sustain Energy Rev 2015;43:1199–213. http://dx.doi.org/10.1016/j.rser.2014.12.002.

[13] Gehlin S. Borehole thermal energy storage. In: Rees SJ, editor. Advances in Ground-Source Heat Pump Systems. Woodhead Publishing; 2016, p. 295–327. http://dx.doi.org/10.1016/B978-0-08-100311-4.00011-X.

[14] Cabeza L, Martorell I, Miró L, Fernández A, Barreneche C. 1 - introduction to thermal energy storage (TES) systems. In: Cabeza LF, editor. Advances in Thermal Energy Storage Systems. Woodhead Publishing Series in Energy, Woodhead Publishing; 2015, p. 1–28. http://dx.doi.org/10.1533/9781782420965.1.

[15] Nouri G, Noorollahi Y, Yousefi H. Solar assisted ground source heat pump systems – a review. Appl Therm Eng 2019;163:114351. http://dx.doi.org/10.1016/j.applthermaleng.2019.114351.

[16] Nilsson E, Rohdin P. Performance evaluation of an industrial borehole thermal energy storage (BTES) project – experiences from the first seven years of operation. Renew Energy 2019;143:1022–34. http://dx.doi.org/10.1016/j.renene.2019.05.020.

[17] Gao L, Zhao J, Tang Z. A review on borehole seasonal solar thermal energy storage. Energy Procedia 2015;70:209–18. http://dx.doi.org/10.1016/j.egypro.2015.02.117, International Conference on Solar Heating and Cooling for Buildings and Industry, SHC 2014.

[18] Guo F, Zhu X, Zhang J, Yang X. Large-scale living laboratory of seasonal borehole thermal energy storage system for urban district heating. Appl Energy 2020;264:114763. http://dx.doi.org/10.1016/j.apenergy.2020.114763.

[19] Mogensen P. Fluid to duct wall heat transfer in duct system heat storages. In: Proceedings of International Conference on Subsurface Heat Storage in Theory and Practice. Stockholm, Sweden, June 6-8.. 1983, p. 652–7.

[20] Claesson J, Eskilson P. Conductive heat extraction to a deep borehole: Thermal analyses and dimensioning rules. Energy 1988;13(6):509–27. http://dx.doi.org/10.1016/0360-5442(88)90005-9.

[21] Spitler JD, Gehlin SE. Thermal response testing for ground source heat pump systems—An historical review. Renew Sustain Energy Rev 2015;50:1125–37. http://dx.doi.org/10.1016/j.rser.2015.05.061.

[22] Fujii H, Okubo H, Itoi R. Thermal response tests using optical fiber thermometers. In: Geothermal Resources Council Transactions - GRC 2006 Annual Meeting: Geothermal Resources-Securing Our Energy Future. 30 I, 2006, p. 545–51, GRC 2006 Annual Meeting: Geothermal Resources-Securing Our Energy Future ; Conference date: 10-09-2006 Through 13-09-2006.

[23] Acuña J, Palm B. Distributed thermal response tests on pipe-in-pipe borehole heat exchangers. Appl Energy 2013;109:312–20. http://dx.doi.org/10.1016/j.apenergy.2013.01.024.

[24] Florides GA, Christodoulides P, Pouloupatis P. Single and double U-tube ground heat exchangers in multiple-layer substrates. Appl Energy 2013;102:364–73. http://dx.doi.org/10.1016/j.apenergy.2012.07.035.

[25] Abdelaziz SL, Ozudogru TY, Olgun CG, Martin JR. Multilayer finite line source model for vertical heat exchangers. Geothermics 2014;51:406–16. http://dx.doi.org/10.1016/j.geothermics.2014.03.004.

[26] Liu J, Wang F, Cai W, Wang Z, Li C. Numerical investigation on the effects of geological parameters and layered subsurface on the thermal performance of medium-deep borehole heat exchanger. Renew Energy 2020;149:384–99. http://dx.doi.org/10.1016/j.renene.2019.11.158.

[27] Karabetoglu S, Ozturk ZF, Kaslilar A, Juhlin C, Sisman A. Effect of layered geological structures on borehole heat transfer. Geothermics 2021;91:102043. http://dx.doi.org/10.1016/j.geothermics.2021.102043.

[28] Luo J, Rohn J, Bayer M, Priess A, Xiang W. Analysis on performance of borehole heat exchanger in a layered subsurface. Appl Energy 2014;123:55–65. http://dx.doi.org/10.1016/j.apenergy.2014.02.044.

[29] Gultekin A, Aydin M, Sisman A. Effects of arrangement geometry and number of boreholes on thermal interaction coefficient of multi-borehole heat exchangers. Appl Energy 2019;237:163–70. http://dx.doi.org/10.1016/j.apenergy.2019.01.027.

[30] Panno D, Buscemi A, Beccali M, Chiaruzzi C, Cipriani G, Ciulla G, Di Dio V, Lo Brano V, Bonomolo M. A solar assisted seasonal borehole thermal energy system for a non-residential building in the mediterranean area. Sol Energy 2019;192:120–32. http://dx.doi.org/10.1016/j.solener.2018.06.014.

[31] Welsch B, Rühaak W, Schulte DO, Bär K, Sass I. Characteristics of medium deep borehole thermal energy storage. Int J Energy Res 2016;40(13):1855–68. http://dx.doi.org/10.1002/er.3570.

[32] Lundh M, Dalenbäck J-O. Swedish solar heated residential area with seasonal storage in rock: Initial evaluation. Renew Energy 2008;33(4):703–11. http://dx.doi.org/10.1016/j.renene.2007.03.024.

[33] Wołoszyn J. Global sensitivity analysis of borehole thermal energy storage efficiency on the heat exchanger arrangement. Energy Convers Manage 2018;166:106–19. http://dx.doi.org/10.1016/j.enconman.2018.04.009.

[34] gçe Başer T, McCartney JS. Transient evaluation of a soil-borehole thermal energy storage system. Renew Energy 2020;147:2582–98. http://dx.doi.org/10.1016/j.renene.2018.11.012, Shallow Geothermal Energy Systems.

[35] Bidarmaghz A, Narsilio GA, Johnston IW, Colls S. The importance of surface air temperature fluctuations on long-term performance of vertical ground heat exchangers. Geomech Energy Environ 2016;6:35–44. http://dx.doi.org/10.1016/j.gete.2016.02.003, Themed Issue on Selected Papers Symposium of Energy Geotechnics 2015 — Part I.

[36] Ma Q, Wang P, Fan J, Klar A. Underground solar energy storage via energy piles: An experimental study. Appl Energy 2022;306:118042. http://dx.doi.org/10.1016/j.apenergy.2021.118042.

[37] Mitchell MS, Spitler JD, Gehlin SEA. Use of cross g-functions to calculate interference between ground heat exchangers used in ground-source heat pump systems. In: World Geothermal Congress. Reykjavik, Iceland: International Geothermal Association; 2020.

[38] Rees S. Advances in Ground Source Heat Pump Systems. Woodhead Publishing; 2016, http://dx.doi.org/10.1016/C2014-0-03840-3.

[39] Aydin M. A new thermal response method for ground heat exchangers and parametric investigation of their performance (Ph.D. thesis), Istanbul Technical University; 2015.

[40] Awrejcewicz J. Numerical Validation Methods. IntechOpen; 2011, http://dx.doi.org/10.5772/1829.

[41] Hahn D, Özisik M. Separation of Variables in the Cylindrical Coordinate System-CH4. Wiley; 2012, http://dx.doi.org/10.1002/9781118411285.ch4.

[42] Zang H, Diao N, Fang Z. A model of finite-length linear heat-source for the vertical embedded pipe of a ground-source heat pump. J Eng Therm Energy Power 2003;104:166–70.

[43] Bandos TV, Campos-Celador Á, López-González LM, Sala-Lizarraga JM. Finite cylinder-source model for energy pile heat exchangers: Effect of buried depth and heat load cyclic variations. Appl Therm Eng 2016;96:130–6. http://dx.doi.org/10.1016/j.applthermaleng.2015.11.073.

[44] Ozisik M. Heat Conduction. Wiley-Interscience publication, Wiley; 1993.